Blind sorting of multiple FH signals in synchronous networking under underdetermined conditions

Yinsong Yang*, *Tao* Wu, *Hui* Wang, *Jinyu* Wang and *Zhiwei* Zhang

Air Force Communication NCO Academy, Dalian 116100, China

Abstract. In order to improve the performance of network sorting under underdetermined conditions, this paper proposes a blind sorting method for multiple frequency hopping (FH) signals in synchronous networking based on the blind source separation. Firstly, the short-time Fourier transform is performed on the multiple FH signals received by the L-shaped antenna array, and the time-frequency map is denoised by using the adaptive threshold of the SNR. Then the time-frequency single-source-point (SSP) detection algorithm is used to get effective time-frequency SSP. The FH signal is segmented on the time-frequency diagram to detect the frequency hopping time. In a certain hopping time, carrier frequency and its corresponding mixing matrix is estimated. Finally, the DOA information of the FH signal is calculated according to the carrier frequency information and the estimated mixing matrix, and the multiple FH signals are sorted according to the DOA information. Theoretical research shows that multiple FH signals can be separated by only three receiving antennas, and simulation results verify the effectiveness of the proposed algorithm.

Keywords: Underdetermined blind source separation, Frequency hopping signal, Network station sorting, DOA.

1 Introduction

Frequency hopping communication is widely used in military communications because of its strong anti-interference, low interception and strong networking capabilities [1]. In order to obtain useful information of the enemy in the communication confrontation, the network station sorting of multiple FH signals is an important task. Hopping period, frequency sets and DOA information are important for FH signal network station sorting [2], especially spatial DOA information, which is the main basis for the separation of synchronous frequency hopping signals.

The existing network station sorting methods usually estimate the characteristic parameters of the FH signals, and then performs clustering and sorting based on the characteristic parameters, but those methods generally require that the number of receiving array elements is more than FH signals. In recent years, the blind source separation algorithm

* Corresponding author: yangyinsong131@163.com

can separate the source signal only by performing certain processing on the observed signal because it can know little about the prior knowledge. It has been widely used in speech aliasing signal separation, biomedical engineering, image processing, mechanical fault detection and other fields [3], so it has also led many scholars to explore its application in frequency hopping signal sorting. Yang Xiao-niu first analyzed the feasibility of blind source separation in FH signal sorting and CDMA multi-user separation in [4]. Subsequently, Fu Wei-hong has greatly developed the application of blind source separation in mixed signal separation in [5,6,7], such as CDMA multi-user separation, communication complex signal separation, and parameter blind estimation and blind sorting of FH signals. [8] proposed the Fast ICA algorithm to separate the aliased FH signals based on the independence of FH signals, but only for receiving array elements more than or equal the number of source signals, it is not applicable to the underdetermined condition. Based on the sparsity of FH signals in the time-frequency domain, [9] used the improved K-means clustering algorithm to estimate the mixing matrix, and then the subspace algorithm and signal relative power are used to separate the source signals. Simulation shows that the algorithm can achieve separation between the synchronous FH signal network platform and the asynchronous FH network station, but does not consider that the hybrid matrix is time-varying. On the basis of the [9], [10] improved the time-frequency single source point detection method and the clustering algorithm respectively, and improved the estimation performance of the algorithm at low SNR, but still did not consider the hybrid matrix is Changed. In [11], a blind separation algorithm for FH signals based on density clustering is proposed. The detailed analysis and experimental simulation of the FH signals are orthogonal and whether there is collision, but the algorithm requires that the energy difference of mixed multi-frequency hopping signals is large enough to satisfy the cluster center surrounded by locally high data. [12,13] considered the problem that the coefficients in the mixing matrix are complex numbers, and proposed a new time-frequency SSP detection method, but the algorithm uses a fixed threshold method to remove noise, estimated performance of the matrix is not good at low SNR. [14] improved the time-frequency SSP detection method. First, the FH signal is segmented by detecting the frequency hopping time, and then estimates the mixing matrix of each segment to obtain DOA information based on the sparse component. Finally performs clustering and splicing to recover the source signal according to the DOA information of each segment. The disadvantage is that the scholar think it can realize denoising and detect SSP synchronously when detecting the time-frequency SSP, so there is no preprocessing for noise. The actual simulation results show that the detection method will mistake some noise points as SSP, especially when the noise interference is relatively large, the performance is less robust.

In summary, this paper proposes a multiple FH signals network station sorting method based on adaptive threshold to denoise and time-frequency SSPs detection. The remainder of this paper is organized as follows: Sect. 2 introduces the data model of FH signals. In Sect. 3, the proposed algorithm for adaptive threshold of the SNR and SSP detection is derived. The experimental results are given in Sect. 4, and finally conclusions are drawn in Sect. 5.

2 The basic model

Firstly, assumed that there are K far-field FH signals received by an L-shaped array with $2M-1$ sensors, and model is shown in Fig.1. The array consists of two ULAs connected orthogonally at one end of each ULA. d is the sensor spacing. The two-dimensional DOA of the kth source is of FH signal is (θ_k,φ_k) ,where θ_k and φ_k denote the azimuth and elevation, respectively. To avoid phase ambiguity, the angles are set to $\theta_k \in [0,\pi/2]$ and $\varphi_k \in [0,\pi]$, respectively.

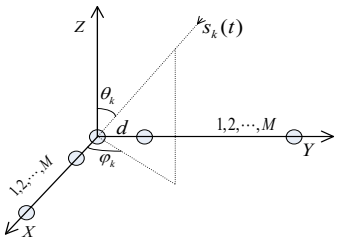

Fig. 1. L-shaped array with 2M − 1 sensors.

We set the origin of the array as the reference sensor, considering transmission delays between source signals to each sensor, and then the *m*th sensor receives the mixed signals and can be described as

$$\begin{aligned} x_m(t) &= \sum_{k=1}^{K} \mu_{mk} s_k(t-\tau_{mk}) + v_m(t) \\ &= \sum_{k=1}^{K} \mu_{mk} s_k(t) e^{-2\pi f_k(t)\tau_{mk}} + v_m(t) \end{aligned} \tag{1}$$

Where μ_{mk} is the amplitude attenuation, τ_{mk} is the transmission delays, $f_k(t)$ is the carrier frequency of *k*th FH signal at the *t* moment.

For the L-shaped array, the time delays at the X and Y sub-arrays are $\tau_{mk}^{x}=d(m-1)\cos\varphi_k \sin\theta_k / c$ and $\tau_{mk}^{y}=d(m-1)\sin\varphi_k \sin\theta_k / c$, respectively. Ignoring the effects of amplitude attenuation and array channel inconsistency, equation (1) can be described in matrix form as

$$\begin{cases} \boldsymbol{x}^x(t) = \boldsymbol{A}^x(t)\boldsymbol{s}(t) + \boldsymbol{v}(t) \\ \boldsymbol{x}^y(t) = \boldsymbol{A}^y(t)\boldsymbol{s}(t) + \boldsymbol{v}(t) \end{cases} \tag{2}$$

Where $\boldsymbol{x}^x(t) = [x_1^x(t), x_2^x(t), ..., x_M^x(t)]^T$ and $\boldsymbol{x}^y(t) = [x_1^y(t), x_2^y(t), ..., x_M^y(t)]^T$ are the observed signals at X and Y sub-arrays. $\boldsymbol{s}(t) = [s_1(t), s_2(t), ..., s_K(t)]^T$ represents the source signals. $\boldsymbol{v}(t)$ represent the Gaussian white noise, Mixing matrices produced by time delays at X and Y sub-arrays are $\boldsymbol{A}^x(t)$ and $\boldsymbol{A}^y(t)$ .we defined $a_{mk}^x(t)$ and $a_{mk}^y(t)$ to represent the (m,k)th elements of $\boldsymbol{A}^x(t)$ and $\boldsymbol{A}^y(t)$, respectively. get the new expression as

$$\boldsymbol{X}(t) = \boldsymbol{A}(t)\boldsymbol{s}(t) + \boldsymbol{V}(t) \tag{3}$$

Where $\boldsymbol{A}(t) = \left[\boldsymbol{A}_1^x(t), ..., \boldsymbol{A}_M^x(t), \boldsymbol{A}_2^y(t), ..., \boldsymbol{A}_M^y(t)\right]^T$, $\boldsymbol{X}(t) = [\boldsymbol{x}_1^x(t), ..., \boldsymbol{x}_M^x(t), \boldsymbol{x}_2^y(t), ..., \boldsymbol{x}_M^y(t)]^T$, $\boldsymbol{V}(t)$ represents the Gaussian white noise data vector.

In order to meet the sparsity requirements of the SAC algorithm, the FH signals are firstly subjected to linear time-frequency transform. In this paper, STFT transform is used as the time-frequency analysis method of the system. STFT processing is performed on both ends of equation (3) can be expressed as

$$\boldsymbol{X}(t,f) = \boldsymbol{A}(t)\boldsymbol{S}(t,f) + \boldsymbol{V}(t,f) \tag{4}$$

From the equation (4), the receiving data model of FH signals can be regarded as a blind

source separation model, which is a hybrid matrix containing DOA information and frequency domain information, which are important basis for network station sorting.

3 The proposed algorithm

3.1 Adaptive threshold with SNR

The influence of ambient noise in the reconnaissance of FH signals is difficult to avoid. Before detecting the time-frequency SSPs, the pre-processing is used to eliminate the noise, and the threshold is ε. The absolute value of the amplitude of the time-frequency point is smaller than the noise of the time-frequency point. which is

$$X(t_i, f_j) = \begin{cases} X(t_i, f_j) & \left|X(t_i, f_j)\right| > \varepsilon \\ 0 & \left|X(t_i, f_j)\right| \le \varepsilon \end{cases} \tag{5}$$

It can be seen that the selection of the threshold is very critical. In this paper, we propose to use the threshold of adaptive change of SNR to denoise. The adaptive threshold calculation steps are as follows. First, we defined the maximum value and the minimum value of the absolute values of all time-frequency points (TFPs) amplitudes on the time-frequency map, calculating the mean value of which are $\varepsilon_{\max}$ and $\varepsilon_{\min}$ as the initial threshold. Then divide the TFPs into the time-frequency domain 1 and the time-frequency domain 2 by using the initial threshold. Calculating the means of the amplitude modulus of the time-frequency domain, respectively.

$$\begin{cases} \varepsilon_{TF1} = \sum\limits_{X(t,f)\in TF1} \varepsilon_{tf} / N_{tf1} \\ \varepsilon_{TF2} = \sum\limits_{X(t,f)\in TF2} \varepsilon_{tf} / N_{tf2} \end{cases} \tag{6}$$

Where N_{tf1} and N_{tf2} are the total number of non-zero TFPs on TF domain 1 and time-frequency domain 2, respectively. Take the mean of the sum as the new threshold which is ε_1, and then iteratively update the threshold according to the above method, repeat it multiple times. Stop iterating when $\left|\varepsilon_{k+1} - \varepsilon_k\right| < 0.1$, and get $\varepsilon = \varepsilon_k$.

3.2 Time-frequency single source point detection

Ignoring the influence of noise, there are some TFPs in the frequency domain. The energy values of the TFPs are only from a certain frequency-hopping source. These TFPs are called time-frequency SSPs. By comparing these time-frequency single sources. The values of the different receiving antennas can be used to obtain an estimate of the mixing matrix. Equation (4) can be expressed as

$$\begin{aligned} \boldsymbol{X}(t,f) &= [\boldsymbol{a}_1(t), \boldsymbol{a}_2(t), \cdots, \boldsymbol{a}_K(t)][S_1(t), S_2(t), \cdots, S_K(t)]^T \\ &= \boldsymbol{a}_1(t)S_1(t) + \boldsymbol{a}_2(t)S_2(t) + \cdots + \boldsymbol{a}_K(t)S_K(t) \end{aligned} \tag{7}$$

Where $[\boldsymbol{a}_1(t), \boldsymbol{a}_2(t), \cdots, \boldsymbol{a}_K(t)] = \boldsymbol{A}(t)$. Suppose there is a time-frequency SSPs $P(t_p, f_p)$ that only comes from the energy transfer of the $S_k(t)$ .So $S_k(t_p, f_p) \neq 0$ and $S_i(t_p, f_p) = 0 (i \neq k)$, then

equation (7) can be expressed as

$$\boldsymbol{X}(t_p, f_p) = \boldsymbol{a}_k S_k(t_p, f_p) \tag{8}$$

Expand equation (8) to obtain time-frequency data on each receiving array element.

$$\begin{cases} X_1(t_p, f_p) = 1 \cdot S_k(t_p, f_p) \\ X_m(t_p, f_p) = a_{mk} \cdot S_k(t_p, f_p) \end{cases}, 2 \le m \le M \tag{9}$$

Where $X_1(t_p, f_p)$ and $X_m(t_p, f_p)$ represent the STFT coefficients of the reference array element and the *m*th array element of the reference element on the *X* axis or *Y* axis, respectively. And the combination equation (9) is expressed as

$$X_m(t_p, f_p) = a_{mk} \cdot S_k(t_p, f_p) \tag{10}$$

For

$$\left\| \begin{bmatrix} \mathrm{Re}\{X_m(t_p, f_p)\} & \mathrm{Im}\{X_m(t_p, f_p)\} \\ -\mathrm{Im}\{X_m(t_p, f_p)\} & \mathrm{Re}\{X_m(t_p, f_p)\} \end{bmatrix}^{-1} \cdot \begin{bmatrix} \mathrm{Re}\{X_1(t_p, f_p)\} \\ \mathrm{Im}\{X_1(t_p, f_p)\} \end{bmatrix} \right\|_2 - 1 \Bigg| < u \tag{11}$$

Where $0 < u < 1$. It is the time-frequency point $P(t_p, f_p)$ if equation (13) is satisfied. This equation can be determined which is one of time-frequency SSPs.

3.3 Mixed matrix and DOA estimation

Assume that the source signal $s_k(t)$ has a set of all time-frequency SSPs G_{kl} in the lth hop, and the total number is L, taking the array element on the X axis as an example. For any $(t_a, f_a) \in G_{kl}$, according to equation (9), we get

$$\frac{X_2^x(t_a, f_a)}{X_1(t_a, f_a)} = \frac{a_{2k}^x(l) s_k(t_a, f_a)}{a_{1k}(l) s_k(t_a, f_a)} = a_{2k}^x(l) = e^{\frac{-j2\pi d f_k(l)}{c} \cos\varphi_k \sin\theta_k} \tag{12}$$

Where $a_{1k}(l)$ is the first row and *k*th column coefficient of the mixing matrix, and the modulus values are all equal to 1.

It can be known from the equation (14) that $a_{2k}^x(l)$ is the ratio of the received time of the reference array element and the second array element on the axis after the STFT and the time-frequency SSPs of the cluster is obtained as an average value. $\boldsymbol{A}^x(l)$ is a vandermonde matrix, so getting $a_{2k}^x(l)$ is equivalent to the estimated value of $\boldsymbol{A}^x(l)$ .Similarly, in the Y axial direction, the following equation is obtained.

$$\frac{X_2^y(t_a, f_a)}{X_1(t_a, f_a)} = \frac{a_{2k}^y(l) s_k(t_a, f_a)}{a_{1k}(l) s_k(t_a, f_a)} = a_{2k}^y(l) = e^{\frac{-j2\pi d f_k(l)}{c} \sin\varphi_k \sin\theta_k} \tag{13}$$

Therefore, the ratio of time-frequency SSPs of two receiving elements is clustered as the average value to obtain $a_{2k}^y(l)$, and then $\boldsymbol{A}^y(l)$ is obtained. In summary, the estimated value of the mixing matrix can be obtained based only on the data received by the three receiving antenna elements.

Considering that the absolute values of the coefficients in the mixing matrix are all equal to 1, the difference between many coefficients is extremely small, and the time-frequency point ratio hash points are aliased together, and the clustering algorithm with better performance cannot separate them. In order to solve this problem, this chapter proposes to estimate the carrier frequency on the time-frequency diagram after the time-frequency single source point detection. The time-frequency point ratio clustering is classified according to the same carrier frequency. The literature [1] gives a carrier frequency estimation method based on time-frequency diagram. The data on the time-frequency diagram has a large amplitude value near the carrier frequency of the frequency hopping signal and has the largest amplitude value at the carrier frequency. The cluster value at each time sampling point is much larger than the frequency value corresponding to the time-frequency point of other points, and the carrier frequency estimation value can be obtained, that is

$$\tilde{f}_k(l) = \sum_{i=1}^{N_l} f_k^{(i)}(l) \Big/ N_l \tag{14}$$

Where N_l is the number of samples in the lth hopping time of the kth hopping signal. Therefore, the estimated equation for DOA is

$$\tilde{\varphi}_k = \begin{cases} \arctan \dfrac{\tilde{f}_k^y(l)\sin\varphi_k \sin\theta_k}{\tilde{f}_k^x(l)\cos\varphi_k \sin\theta_k} + \pi & \text{if } \tilde{f}_k^x(l)\cos\varphi_k \sin\theta_k < 0 \\ \pi/2 & \text{if } \tilde{f}_k^x(l)\cos\varphi_k \sin\theta_k = 0 \\ \arctan \dfrac{\tilde{f}_k^y(l)\sin\varphi_k \sin\theta_k}{\tilde{f}_k^x(l)\cos\varphi_k \sin\theta_k} & \text{others} \end{cases} \tag{15}$$

$$\tilde{\theta}_k = \arcsin \frac{\tilde{f}_k^y(l)\sin\varphi_k \sin\theta_k}{\tilde{f}_k^y(l)\sin\tilde{\varphi}_k} \tag{16}$$

For the same hopping signal, the DOA information of each hop is unchanged. Therefore, according to the DOA information, the signals of the respective segments can be spliced together to realize network station sorting.

Table 1. Source signal parameter information.

S(t)	Frequency (MHz)	Hopping period (MS)	DOA
S_1	[8,6,2]	0.8	(10°,150°)
S_2	[6.5,3.5,4]	0.8	(30°,120°)
S_3	[2.5,1,5]	0.8	(50°,80°)
S_4	[4,7,8.5]	0.8	(65°,50°)
S_5	[3,4.5,5.5]	0.8	(85°,20°)

4 Experiment and analysis

This section evaluates the performance of the algorithm through simulation experiments. The experimental conditions are as follows: the number of receiving antennas are 3(M=2), the spacing of array elements is d=5m, and 4 FH signals are received at the same time, and the sampling frequency is 20MHz. The parameter settings of the 4 FH signals are shown in Table 1 below.

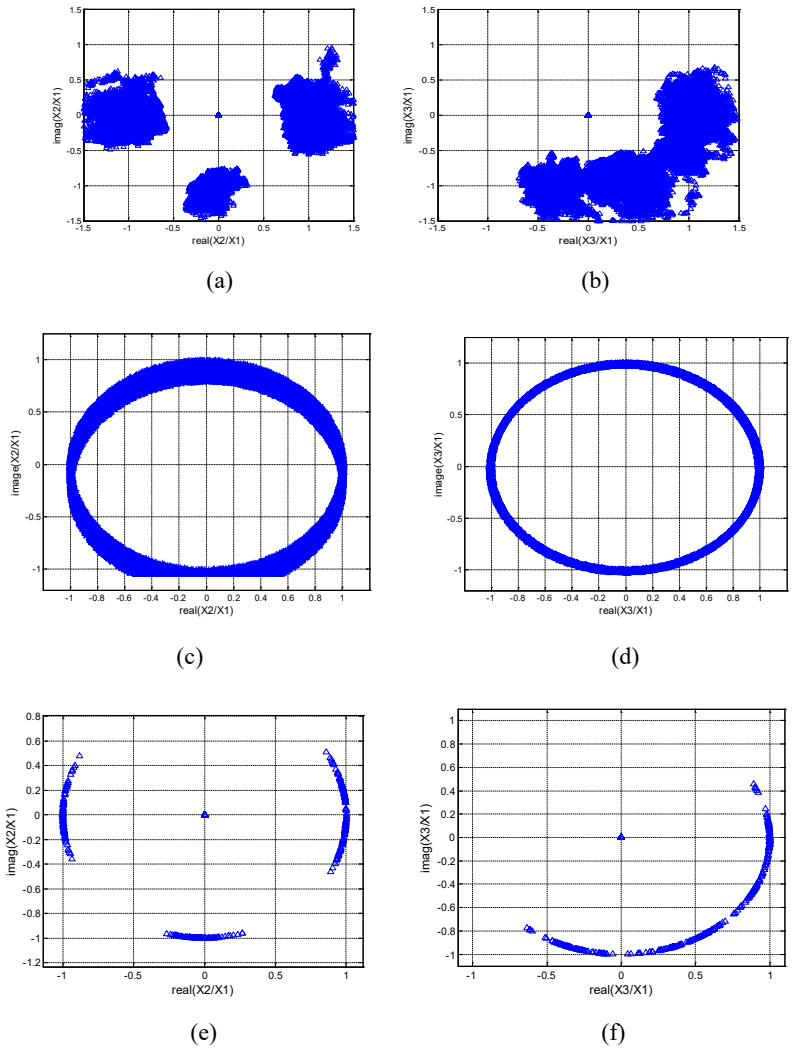

Fig. 2. Time-frequency point ratio hash map under different processing condition.

4.1 Experiment 1

In order to verify the importance of adaptive SNR denoising and time-frequency unit point detection for algorithm post-processing, this experiment simulates the time-frequency point ratio (mixed matrix coefficient) hash map distribution of observed signals under different processing methods. analysis. The experimental conditions are set to: the signal to noise ratio is 0dB, and the FH signals consist of S_1, S_2, S_3, S_4. The threshold for time-frequency single source detection is set to $u = 0.01$, and the mixing matrix is

In Fig. 2, (a) and (b) are obtained by the algorithm in [11-13], and the time-frequency points after noise removal are regarded as time-frequency single source points. (c) and (d) are obtained by the algorithm in reference [2,3], and the threshold is set to remove the non-time-frequency single source point directly without denoising. (e) and (f) are obtained by the algorithm proposed in this chapter.

$$\boldsymbol{A} = \begin{bmatrix} 1.0000 + 0.0000i & 1.0000 + 0.0000i & 1.0000 + 0.0000i & 1.0000 + 0.0000i \\ -1.0000 - 0.0046i & -0.0154 - 0.9999i & 0.9659 + 0.2588i & 0.9876 - 0.1568i \\ 0.4160 - 0.9094i & -0.3141 - 0.9494i & 0.8989 - 0.4381i & 0.9959 + 0.0908i \end{bmatrix}$$

The simulation result graph shows that if the time-frequency diagram is not firstly subjected to noise removal processing, direct time-frequency single-source point detection will mistake many noise points as single source points, causing the effective time-frequency point ratio to be submerged in the noise time-frequency point ratio. Therefore, it is necessary to remove the noise interference before the single source point detection.

4.2 Experiment 2

In the case of a fixed SNR, Figure3 shows the MSE value of the mixing matrix as a function of different u . Figure 4 shows the RMSE of the DOA estimate as a function of u .

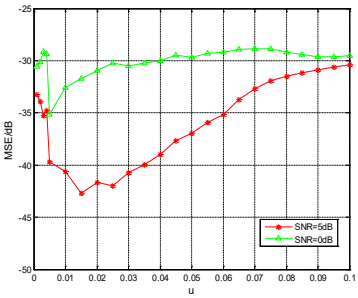

Fig. 3. MSE changes with u .

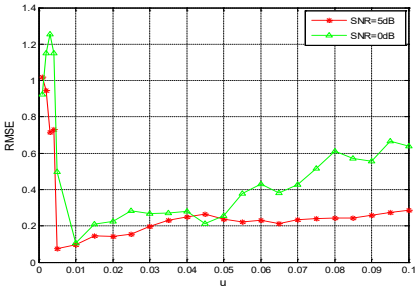

Fig. 4. RMSE changes with u .

It can be seen that under certain conditions of SNR when the u is small, the estimation performance of the mixed matrix and DOA becomes better as the u increases; when the u is large to a certain extent, the estimated performance deteriorates with the increase of the u .It can be seen that the estimated performance of the algorithm in this chapter is the best around 0.01.

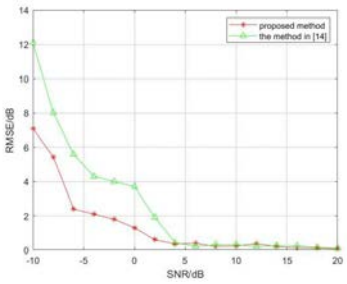

Fig. 5. RMSE changes with SNR.

Fig.5 shows the RMSE of the DOA estimate as a function of SNR, where $u = 0.01$. The simulation results show that the RMSE of the DOA estimates obtained by the algorithm in this chapter is significantly smaller than that in the literature [14] when the SNR is lower than 5dB, which indicates that the proposed algorithm has better estimation performance at low SNR. However more than 5dB, the DOA estimation performance of the proposed algorithm is similar to that of the algorithm in [14].

5 Conclusion

The theoretical analysis and simulation results show that the proposed algorithm can separate four frequency hopping signal sources with the number of array elements being 3, and the performance of the algorithm in this chapter is better than the reference algorithm.

References

1. FU W, HEI Y, LI X. UBSS and blind parameters estimation algorithms for synchronous orthogonal FH signals [J]. Journal of Systems Engineering and Electronics, 2014, 25(6):911-920.
2. GUO X, TIAN Y, LI Y. A mixing matrix estimation algorithm for frequency hopping signals under the UBSS model [C]. 2017 Progress in Electromagnetics Research Symposium - Fall (PIERS - FALL).
3. GUO Q, RUAN G, QI L. A Complex-Valued Mixing Matrix Estimation Algorithm for Underdetermined Blind Source Separation [J]. Circuits Systems & Signal Processing, 2018(7):1-21.
4. YANG X N, FU W H. Blind Source Separation: Theory, Application and Prospect [J]. COMMUNICATION COUNTERMEASURES, 2006(03):3-10.
5. FU W H, WU S H, LIU A J, et al. Underdetermined Blind Source Separation of Frequency Hopping Signal [J]. Journal of Beijing University of Posts and Telecommunications, 2015(06):11-14.
6. FU W H, WU S H, ZHANG F L, et al. A Blind Parameter Estimation Algorithm of Fast Frequency Hopping Signals for Underdetermined Situation Based on ARMA Model [J]. Journal of Beijing University of Posts and Telecommunications, 2014(05):16-19.
7. FU W H, ZHAONG Z B, YI B. The Research of SCBSS Technology: Survey and Prospect [J]. Journal of Beijing University of Posts and Telecommunications, 2017(05):1-11.
8. CHENG C, GAO X J, LI D X. Overlapped Frequency-Hopping Communication Signals Separation Algorithm Based on Independent Component Analysis [J]JOURNAL OF JILIN UNIVERSITY (INFORMATION SCIENCE EDITION) 2008(04):347-351.
9. SHA Z C, HUANG Z T, ZHOU Y Y, et al. Frequency-hopping signals sorting based on underdetermined blind source separation[J] IET communications,2013,7(14):1456-1464.
10. YU X Y, GUO Y, ZHANG K F, et al. A Network Sorting Algorithm Based on Blind Source Separation of Multi-FH Signal [J]. Journal of Signal Processing, 2017(08):1082-1089.
11. LI C, ZHU L, ZHANG Z. Non-orthogonal frequency hopping signal underdetermined blind source separation in time-frequency domain [J]. 2016.
12. LI H, SHEN Y H, WANG J G, et al. Estimation of the complex-valued mixing matrix by single-source-points detection with less sensors than sources [J]. European Transactions on Telecommunications, 2012, 23(2):137-147.
13. LI Y, NIE W, YE F. A Complex Mixing Matrix Estimation Algorithm Based on Single Source Points [J]. Circuits Systems & Signal Processing, 2015, 34(11):3709-3723.
14. ZHANG C, WANG Y, JING F. Underdetermined Blind Source Separation of Synchronous Orthogonal Frequency Hopping Signals Based on Single Source Points Detection[J]. Sensors, 2017, 17 (9).